

# Motion-induced synchronization in metapopulations of mobile agents

Jesús Gómez-Gardeñes,<sup>1,2</sup> Vincenzo Nicosia,<sup>3</sup> Roberta Sinatra,<sup>4</sup> and Vito Latora<sup>5</sup>

<sup>1</sup>*Departamento de Física de la Materia Condensada, University of Zaragoza, Zaragoza 50009, Spain*

<sup>2</sup>*Institute for Biocomputation and Physics of Complex Systems (BIFI), University of Zaragoza, Zaragoza 50018, Spain*

<sup>3</sup>*Computer Laboratory, University of Cambridge, Cambridge CB3 0FD, United Kingdom*

<sup>4</sup>*Center for Complex Network Research and Department of Physics,  
Northeastern University, Boston, Massachusetts 02115, USA*

<sup>5</sup>*School of Mathematical Sciences, Queen Mary University of London, London E1 4NS, United Kingdom*

(Dated: June 13, 2012)

We study the influence of motion on the emergence of synchronization in a metapopulation of random walkers moving on a heterogeneous network and subject to Kuramoto interactions at the network nodes. We discover a novel mechanism of transition to macroscopic dynamical order induced by the walkers' motion. Furthermore, we observe two different microscopic paths to synchronization: depending on the rules of the motion, either low-degree nodes or the hubs drive the whole system towards synchronization. We provide analytical arguments to understand these results.

PACS numbers: 05.45.Xt, 89.75.-k

The spontaneous emergence of synchronization in systems of coupled dynamical units [1, 2] underlies the development of coordinated tasks as diverse as metabolic cycles in eukaryote cells, cognitive processes in the human brain and opinion formation in social systems [3–5]. In the last decade complex networks theory has revealed that the topology of the interactions in a complex system has important effects on its collective behavior [6, 7]. As a consequence, many recent studies have considered dynamical systems coupled through non-trivial topologies [8], uncovering the impact of the structural patterns on the existence [9–13] and stability [14–17] of synchronized states. Most of the times, the interaction patterns keep changing over time. Their evolution can either be driven by the synchronization process itself, as in models of dynamically adapting networks [18–21], or be determined by the fact that each unit moves at random over a continuous and homogeneous space and interacts only with other units within a given distance [22–25]. However, the movements of agents in the real world usually take place on heterogeneous networks, and are characterized by long-range correlations [26–28]. These factors have an impact on the emergence of collective behaviours in general, and of synchronization in particular. For these reasons, metapopulation modeling has been successfully exploited in different contexts, including the study of epidemic spreading and chemical reactions [26, 27, 29–32].

In this letter we study the emergence of synchronization in a metapopulation model which incorporates mobility over a complex network together with local interactions of the agents at the network nodes. The evolution of the metapopulation model is then driven by the interplay of two concurrent dynamical processes: the interaction between agents on the same node, which affects the time evolution of their internal dynamical state, and the movement of agents at the network level, which changes the pattern of interactions. We discover, in fact, a novel

mechanism of synchronization that we name *motion-induced synchronization*, since the transition from disorder to macroscopic order is controlled by the value of the parameter tuning the motion. Furthermore, we show that there are two different types of microscopic mechanisms driving the system towards synchronization, according to whether the walkers prefer to visit or to avoid high-degree nodes.

In our metapopulation model, the first (bottom) level consists of a set of  $W$  mobile agents (walkers). Each agent  $i$  ( $i = 1, 2, \dots, W$ ) is a dynamical system whose state at time  $t$  is described by a phase variable,  $\theta_i(t) \in [0, 2\pi)$ , and changes over time as a result of the interaction with other agents. At the second (top) level there is a complex network with  $N$  nodes and  $E$  edges, described by the adjacency matrix  $\mathcal{A}$ , whose entry  $a_{IJ}$  is equal to 1 if nodes  $I$  and  $J$  are connected, and 0 otherwise (here and in the following we indicate nodes of the graph in uppercase letters, and walkers in lowercase). Agents move and interact over the network. Assume that, at a given time  $t$ , we have  $i \in I$ , *i.e.* agent  $i$  is at node  $I$ . The evolution of the phase  $\theta_i(t)$  of agent  $i$  is ruled by Kuramoto interactions with all the other walkers being on the same node at time  $t$  [3, 33, 34]:

$$\dot{\theta}_i(t) = \omega_i + \lambda \sum_{j \in I} \sin(\theta_j(t) - \theta_i(t)), \quad \forall i \in I, \quad I = 1, \dots, N \quad (1)$$

where  $\omega_i$  is the internal frequency of agent  $i$ , and  $\lambda$  is the control parameter accounting for the strength of the interaction between walkers. The internal frequencies of the agents are randomly drawn from a uniform distribution  $g(\omega) = 1/2$  in the interval  $\omega_i \in [-1, 1]$ .

At regular time intervals of length  $\Delta$  the agents perform one step of a *degree-biased* random walk. Namely, we assume that a walker at node  $I$  moves to a node  $J$

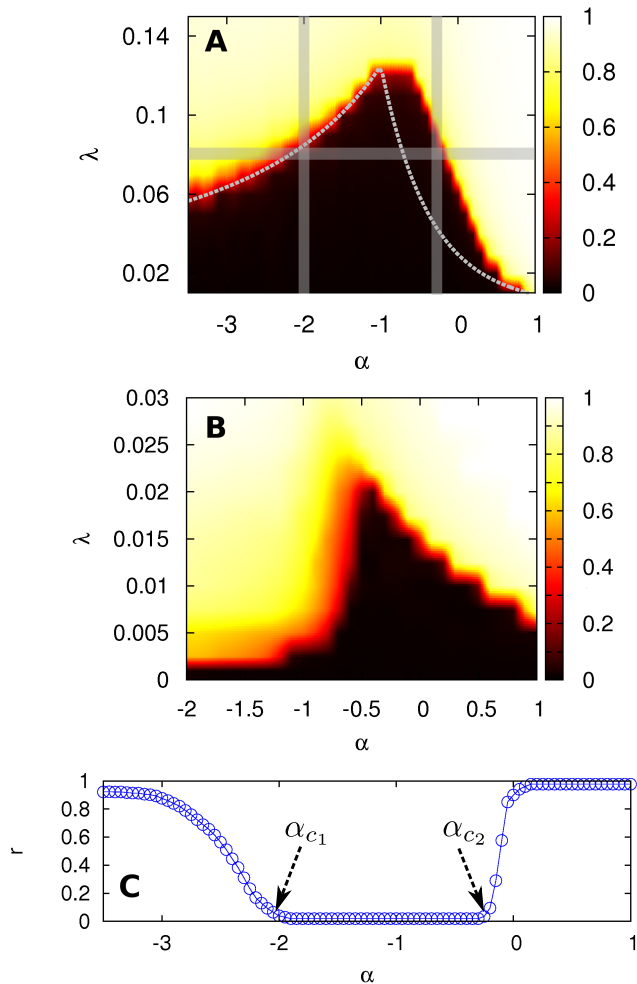


FIG. 1. (color online) Phase diagram  $r(\alpha, \lambda)$  of the metapopulation model on uncorrelated SF networks with  $\gamma = 3$  (panel A) and on the US air-transportation network (panel B). Both networks have  $N = 500$  nodes. The dashed curve in the first panel is a lower-bound analytical prediction for the onset of synchronization in uncorrelated graphs obtained from Eq. (8) for  $\alpha > -1$ , and from Eq. (9) for  $\alpha < -1$ . Panel C shows  $r(\alpha)$  for  $\lambda = 0.08$ , corresponding to the horizontal line in panel A.

with a probability proportional to  $k_J$  [36, 37]:

$$\Pi_{I \rightarrow J} = \frac{a_{IJ} k_J^\alpha}{\sum_{L=1}^N a_{IL} k_L^\alpha}, \quad (2)$$

where  $\alpha$  is a tunable parameter which biases agents' motion either towards low-degree nodes ( $\alpha < 0$ ) or towards hubs ( $\alpha > 0$ ). For  $\alpha = 0$ , we recover the standard (unbiased) random walk. In summary, the metapopulation model has three control parameters:  $\lambda$  regulating the interaction strength between walkers,  $\alpha$  tuning the rule of their motion, and  $\Delta$  fixing the ratio between the time scales of the two concurrent dynamical processes (the Kuramoto dynamics and the motion over the graph).

As usual in the Kuramoto model, the degree of syn-

chronization of the whole metapopulation at time  $t$  is measured by means of the global order parameter:

$$r(t) = \left| \frac{1}{W} \sum_{i=1}^W e^{i\theta_i(t)} \right|, \quad (3)$$

where  $r = 0$  if the phases of the agents are completely incoherent, while  $r = 1$  when the system is fully synchronized. In order to quantify the degree of synchronization of a single node  $I$  we introduce the local order parameter:

$$r_I(t) = \left| \frac{1}{w_I(t)} \sum_{i \in I} e^{i\theta_i(t)} \right|, \quad I = 1, 2, \dots, N \quad (4)$$

where  $w_I(t)$  is the number of agents at node  $I$  at time  $t$ . When the phases of the walkers at node  $I$  are fully synchronized, the local order parameter of the node is equal to 1, while in the case of complete disorder  $r_I = 0$ .

In order to investigate the effects of motion on the emergence of synchronization we have simulated the metapopulation model on various synthetic networks and, as an example of a real complex network, on the US air-transportation system. This network describes the connections, via commercial flights, between the  $N = 500$  largest airports in the US and, due to its intrinsic nature as a backbone for human transportation, has already been used to investigate reaction-diffusion dynamics in metapopulation models [26]. Since this network has a long-tailed degree distribution and exhibits degree-degree correlations, we have generated, for comparison, uncorrelated scale-free (SF) networks with  $N = 500$  nodes and a power-law degree distribution  $P(k) \sim k^{-\gamma}$  with a tunable value of the exponent  $\gamma$  [35]. The numerical simulations of the model have been performed by starting from a stationary distribution of  $W = 5000$  walkers over the networks [36], and by integrating the equation of motion for a time  $t_0 = m\Delta$ , where  $m = 10^4$  is the number of random walk steps performed. After this transient, we measured global and local degree of synchronization,  $r$  and  $r_I$  for  $I = 1, \dots, N$ , by respectively averaging the values of  $r(t)$  and  $r_I(t)$  in Eq. (3) and Eq. (4) over a time window of length  $T = 2m\Delta$ .

In Fig. 1 we show the global order parameter  $r$  as a function of the coupling strength  $\lambda$ , and of the walker bias  $\alpha$ . The two phase diagrams have been obtained with the same value of the parameter fixing the ratio between time scales, namely  $\Delta = 0.05$ . The SF network reported has  $\gamma = 3$ , although similar results have been obtained for other values of the exponent in the range  $2 < \gamma < 3$ .

As expected, by increasing  $\lambda$  at a fixed value of  $\alpha$ , *i.e.* keeping fixed the rules of motion, we observe a phase transition from the incoherent phase ( $r \simeq 0$ , dark regions of the diagrams) to a synchronized state ( $r \neq 0$ , bright regions of the diagrams). However, the precise value for the onset of synchronization, namely the critical value

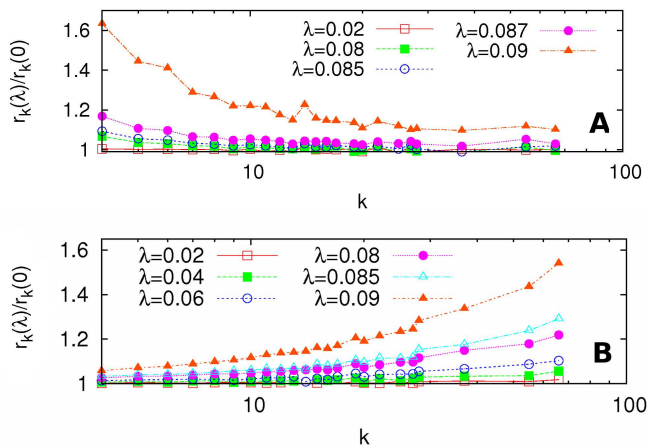


FIG. 2. (color online) The average local order parameter  $r_k$  of nodes of degree  $k$  as a function of  $k$ , for various values of  $\lambda$ , and for two fixed values of the bias, respectively  $\alpha = -2$ . (panel A) and  $\alpha = -0.25$  (panel B), corresponding to the two vertical lines in Fig. 1.A.

$\lambda_c$  where the incoherent state becomes unstable, strongly depends on the motion bias  $\alpha$ . In particular, we find that  $\lambda_c(\alpha)$  is first increasing as function of  $\alpha$ , and then decreasing. The function  $\lambda_c(\alpha)$  reaches its maximum  $\lambda_c^{\max}$  at a particular value of  $\alpha$ , namely at  $\alpha^* \simeq -1$  for the SF network (we have checked that this is true for any value of  $\gamma$  in the interval  $(2, 3]$ ), and at  $\alpha^* \simeq -0.5$  for the air-transportation network. As a consequence of the shape of  $\lambda_c(\alpha)$ , for a wide range of values of the strength  $\lambda$  such that  $\lambda < \lambda_c^{\max}$ , we observe a novel mechanism of *motion-induced* synchronization. This means that we can fix the value of the interaction strength  $\lambda$ , and we can control whether the system is in the incoherent phase ( $r \simeq 0$ , dark regions) or in the synchronized state ( $r \neq 0$ , bright regions) by solely changing the rule of motion.

Let us focus on the case of the SF network shown in Fig. 1.A and suppose to keep  $\lambda$  fixed at 0.08 (see the horizontal line in the figure). As shown in Fig. 1.C, we can start with a value of  $\alpha$  within the incoherent phase, for instance  $\alpha = \alpha^* = -1$ , and consider the behavior of the system as we decrease the value of  $\alpha$ . When  $\alpha$  gets smaller than a particular critical value  $\alpha_{c_1}(\lambda)$ , in this case  $\alpha_{c_1}(0.08) \simeq -2.0$ , we observe a transition from the incoherent to the synchronized phase. Conversely, we can start at  $\alpha = -1$  and get a synchronized state by increasing the motion bias parameter to values larger than  $\alpha_{c_2}(0.08) \simeq -0.2$ . In conclusion, a fine tuning of the rules controlling the agents' motion can effectively produce dramatic changes in the *macroscopic* synchronization state of the system. For any value of  $\lambda < \lambda_c^{\max}$ , we get two critical values of the bias  $\alpha_{c_1}(\lambda) < \alpha^*$  and  $\alpha_{c_2}(\lambda) > \alpha^*$  whose positions depend on  $\lambda$ . This means that, if we start at  $\alpha < \alpha_{c_1}(\lambda)$  and we keep increasing the value of  $\alpha$ , we observe a mechanism of fall-and-rise syn-

chronization induced by motion: the degree of synchronization in the metapopulation model can be tuned from full synchronization to an incoherent state, and back to full synchronization, solely by increasing  $\alpha$ , while keeping fixed  $\lambda$ .

In addition, we have found that the bias in the motion affects the onset of synchronization also at the *microscopic* level. To illustrate our results let us consider two different values of the bias for the case of the model implemented on the uncorrelated SF graph with  $\gamma = 3$ , namely  $\alpha = -2.0 < \alpha^*$  and  $\alpha = -0.25 > \alpha^*$ . We are interested on the microscopic paths to synchronization [11] as we increase  $\lambda$ , by following the two vertical lines shown in Fig. 1.A. In particular, we have computed the value of the local order parameter for each of the nodes of the graph, as in Eq. (4), and we have grouped nodes into degree classes. We obtain an average value for the synchronization of nodes of degree  $k$  as:

$$r_k = \frac{1}{N_k} \sum_{I=1}^N r_I \delta(k_I, k), \quad (5)$$

where  $N_k = NP(k)$  is the number of nodes in the class of degree  $k$ . We report in Fig. 2 the quantity  $r_k(\lambda)$  divided by  $r_k(0)$ , as a function of  $k$ , and for different values of  $\lambda$ . The two panels refer, respectively, to  $\alpha = -2.0$  and to  $\alpha = -0.25$ . While for  $\alpha = -2.0$  the nodes having small degree are the first ones to attain local synchronization as soon as  $\lambda$  crosses the critical value  $\lambda_c(-2.0) \simeq 0.08$ , for  $\alpha = -0.25$ , the hubs are the nodes which synchronize first when  $\lambda > \lambda_c(-0.25) \simeq 0.07$ . We thus observe two microscopic paths to synchronization: either driven by low-degree nodes ( $\alpha < \alpha^*$ ), or by the hubs ( $\alpha > \alpha^*$ ).

We can understand the (macroscopic and microscopic) effects of motion on synchronization by the following analytical argument which allows to derive a lower-bound estimate for  $\lambda_c$  as a function of  $\alpha$  (in the two regimes  $\alpha < \alpha^*$  and  $\alpha > \alpha^*$ ) under the assumption that: (i) the network is uncorrelated and (ii) the phases of the walkers at each given node reach a stationary state before the walkers move to other nodes. The average number  $w_I$  of biased random walkers at a node  $I$  of an undirected and connected graph reads [36, 37]:

$$w_I = \frac{W c_I k_I^\alpha}{\sum_{J=1}^N c_J k_J^\alpha} \simeq \frac{W k_I^{\alpha+1}}{\sum_{J=1}^N k_J^{\alpha+1}} = \frac{W k_I^{\alpha+1}}{N \langle k^{\alpha+1} \rangle}, \quad (6)$$

where  $c_I = \sum_{J=1}^N a_{IJ} k_J^\alpha$  and the symbol  $\langle \cdot \rangle$  denotes the average over all the nodes in the network. Note that the second equality is strictly valid only for networks without degree-degree correlations, as the SF graphs in Fig. 1.A and in Fig. 2. For a given  $\alpha$ , the value  $w_I$  only depends on the connectivity  $k_I$  of the node, so that nodes with the same degree will have the same average number of walkers. Thus, in the following we will indicate as  $w_k$  the

number of agents on a node with degree  $k$ . Note also that if the graph is uncorrelated, a motion rule with  $\alpha = -1$ , *i.e.* a biased random walk in which the walkers move to a node with a probability inversely proportional to its degree, leads to a uniform distribution of the walkers over the nodes, since  $w_I$  in Eq. (6) does not depend on  $k_I$  any more. Now, if assumption (ii) holds true, then for each node  $I$ , we can make use of the expression for the critical coupling for a set of  $w_I$  all-to-all interacting Kuramoto oscillators:  $\lambda_c \cdot w_I = 2/[\pi \cdot g(0)]$  (see [3, 34]). We can therefore write the critical coupling strength for the synchronization of the walkers at a node of degree  $k$  as:

$$\lambda_c(k) = \frac{2}{w_k \pi g(0)} = \frac{4N \langle k^{\alpha+1} \rangle}{W \pi k^{\alpha+1}}, \quad (7)$$

where we have made use of Eq. (6). The expression of  $\lambda_c(k)$  depends on  $W/N$  and on the value of the motion bias  $\alpha$ . Thus, once we have set the values of  $W/N$ ,  $\alpha$  and  $\lambda$ , a node of degree  $k$  will be locally synchronized ( $r_k \neq 0$ ) if  $\lambda_c(k) < \lambda$ .

Equation (7) sheds light on the two different microscopic paths to synchronization observed in Fig. 2. Let us indicate as  $k_{\min}$  and  $k_{\max}$  the minimum and maximum degree in the network. Suppose to consider two values of  $\alpha$ , one larger and one smaller than  $\alpha^* = -1$ , for instance the two values  $\alpha = -2$  and  $\alpha = -0.25$  considered in Fig. 2 and corresponding to the two vertical lines in Fig. 1.A. If we start increasing  $\lambda$  from  $\lambda = 0$ , our arguments predict no local synchronization until  $\lambda$  becomes larger than the smallest  $\lambda_c(k)$ , which corresponds to  $k = k_{\min}$  if  $\alpha < -1$ , or to  $k = k_{\max}$  if  $\alpha > -1$ . At this point, the nodes with the smallest (largest) degree are locally synchronized if  $\alpha < -1$  ( $\alpha > -1$ ). If we keep increasing  $\lambda$ , synchronization is progressively attained also by nodes with larger (resp. smaller) degrees when  $\alpha < -1$  (resp.  $\alpha > -1$ ), as found numerically in Fig. 2. We can therefore derive a lower-bound approximation  $\tilde{\lambda}_c(\alpha)$  of the curve  $\lambda_c(\alpha)$  delimiting the synchronization region ( $r \neq 0$ ), by considering the smallest value of  $\lambda$  at which the first degree-class of nodes becomes locally synchronized. In particular, for a SF network with  $P(k) \sim k^{-\gamma}$ , as the ones used in our simulations, we get:

$$\tilde{\lambda}_c(\alpha) = \frac{4(\gamma - 1) [(k_{\min})^{\gamma-1} - (k_{\min})^{\alpha+1} (k_{\max})^{\gamma-\alpha-2}]}{\pi W (\alpha + 2 - \gamma)}, \quad (8)$$

when  $\alpha > -1$ , and:

$$\tilde{\lambda}_c(\alpha) = \frac{4(\gamma - 1) [(k_{\max})^{\alpha+1} (k_{\min})^{\gamma-\alpha-2} - (k_{\max})^{\gamma-1}]}{\pi W (\alpha + 2 - \gamma)}, \quad (9)$$

for  $\alpha < -1$ . In the particular case when  $\alpha = \alpha^* = -1$  all the nodes in the network have the same average number of agents and they become locally synchronized altogether at  $\lambda = 4N/(W\pi)$ , as can be seen from Eq. (7).

This corresponds to the largest possible value  $\lambda_c^{\max}$  of the critical interaction strength. The curve  $\tilde{\lambda}_c(\alpha)$  predicted by the theory for the same values of  $W/N$ ,  $k_{\min}$  and  $\gamma$  used in the numerical simulations, is reported in Fig. 1.A as dashed line. The theory works quite well in determining the real boundary  $\lambda_c(\alpha)$  in a system with no degree-degree correlations, and also predicts quite accurately the position of the cusp at  $\alpha = \alpha^* = -1$  for any value of  $\gamma$  in (2, 3].

Summing up, our work unveils new factors that can favor or hinder synchronization, other than the strength of the coupling and the structure of the interaction graph. In fact, we have studied a metapopulation model where agents move according to a one-parameter motion rule, showing that the value of such a parameter controls the transition to synchronization. Our results open the door to the study of synchronization in metapopulations and to further investigation of synchrony-driven motion aimed at enhancing or suppressing synchronized states in large and structured populations.

We acknowledge support from the Spanish DGICYT under projects MTM2009-13848 and FIS2011-25167, and by the Comunidad de Aragón (Project No. FMI22/10). J.G.G. is supported by MICINN through the Ramón y Cajal program. R.S acknowledges support from the James S. McDonnell Foundation.

- 
- [1] Pikovsky, A., Rosenblum, M. & Kurths, J. *Synchronization: a Universal Concept in Nonlinear Sciences* (Cambridge University Press, 2003).
  - [2] S. Boccaletti, *The Synchronized Dynamics of Complex Systems* (Elsevier, 2008).
  - [3] S.H. Strogatz, *Physica D* **143**, 1 (2000).
  - [4] E. Bullmore and O. Sporns, *Nature Reviews Neuroscience* **10**, 186 (2009).
  - [5] A. Pluchino, V. Latora, A. Rapisarda, *Internat. J. Modern Phys. C* **16**, 515 (2005).
  - [6] S.H. Strogatz, *Nature* **410**, 268 (2001).
  - [7] S. Boccaletti, V. Latora, Y. Moreno, M. Chavez and D.-U. Hwang, *Phys. Rep.* **424**, 175 (2006).
  - [8] A. Arenas, A. Díaz-Guilera, J. Kurths, Y. Moreno and C. Zhou, *Phys. Rep.* **469**, 93 (2008).
  - [9] Y. Moreno and A.F. Pacheco, *Europhys. Lett.* **68**, 603 (2004).
  - [10] A. Arenas, A. Díaz-Guilera and C.J. Pérez-Vicente, *Phys. Rev. Lett.* **96**, 114102 (2006).
  - [11] J. Gómez-Gardeñes, Y. Moreno and A. Arenas, *Phys. Rev. Lett.* **98**, 034101 (2007).
  - [12] I. Lodato, S. Boccaletti and V. Latora, *Europhys. Lett.* **78**, 28001 (2007).
  - [13] J. Gómez-Gardeñes, S. Gómez, A. Arenas and Y. Moreno. *Phys. Rev. Lett.* **106**, 128701 (2011).
  - [14] T. Nishikawa, A.E. Motter, Y.-C. Lai and F.C. Hoppensteadt, *Phys. Rev. Lett.* **91**, 014101 (2003).

- [15] M. Chavez, D.-U. Hwang, A. Amann, H.G.E. Hentschel and S. Boccaletti, *Phys. Rev. Lett.* **94**, 218701 (2005).
- [16] C. Zhou, A.E. Motter and J. Kurths, *Phys. Rev. Lett.* **96**, 034101 (2006).
- [17] D. Gfeller, P. De Los Rios, *Phys. Rev. Lett.* **100**, 174104 (2008).
- [18] C. Zhou and J. Kurths, *Phys. Rev. Lett.* **96**, 164102 (2006).
- [19] F. Sorrentino and E. Ott, *Phys. Rev. Lett.* **100**, 114101 (2008).
- [20] T. Aoki and T. Aoyagi, *Phys. Rev. Lett.* **102**, 034101 (2009).
- [21] R. Gutierrez, A. Amann, S. Assenza, J. Gómez-Gardeñes, V. Latora and S. Boccaletti, *Phys. Rev. Lett.* **107**, 234103 (2011).
- [22] A. Buscarino, L. Fortuna, M. Frasca, and A. Rizzo, *Chaos* **16**, 015116 (2006).
- [23] M. Frasca, A. Buscarino, A. Rizzo, L. Fortuna, S. Boccaletti, *Phys. Rev. Lett.* **100**, 044102 (2008).
- [24] N. Fujiwara, J. Kurths, and A. Díaz-Guilera, *Phys. Rev. E* **83**, 025101 (2011).
- [25] M. Frasca, A. Buscarino, A. Rizzo, L. Fortuna, *Phys. Rev. Lett.* **108**, 204102 (2012).
- [26] V. Colizza, R. Pastor-Satorras, and A. Vespignani, *Nature Physics* **3**, 276 (2007).
- [27] V. Colizza, A. Barrat, M. Barthélemy, and A. Vespignani, *Proc. Nat. Acad. Sci. USA* **103**, 2015 (2006).
- [28] M. Szell, R. Sinatra, G. Petri, S. Thurner, V. Latora, arXiv:1112.1220 in press in *Scientific Reports*
- [29] V. Colizza and A. Vespignani, *Phys. Rev. Lett.* **99**, 148701 (2007).
- [30] V. Colizza and A. Vespignani, *J. Theor. Biol.* **251**, 450 (2008).
- [31] S. Meloni, A. Arenas and Y. Moreno, *Proc. Nat. Acad. Sci. USA* **106**, 16897 (2009).
- [32] S. Meloni, N. Perra, A. Arenas, S. Gómez, Y. Moreno and A. Vespignani *Scientific Reports* **1**, 62 (2011).
- [33] Y. Kuramoto, *Lect. Notes in Physics* **30**, 420 (1975).
- [34] J.A. Acebrón, L.L. Bonilla, C.J. Pérez-Vicente, F. Ritort and R. Spigler *Rev. Mod. Phys.* **77**, 137 (2005).
- [35] E. A. Bender and E.R. Canfield, *Journ. of Combinatorial Theory* **A24**, 296 (1978)
- [36] J. Gómez-Gardeñes and V. Latora, *Phys. Rev. E* **78**, 065102(R) (2008).
- [37] R. Sinatra, J. Gómez-Gardeñes, R. Lambiotte, V. Nicosia, V. Latora, *Phys. Rev. E* **83**, 030103(R) (2011).